Hydrogen desorption from nanostructured graphite: *ab initio* molecular-dynamics studies

Hydrogen desorption from nanostructured graphite: *ab initio* molecular-dynamics studies

A Harada[1], F Shimojo[2] and K Hoshino[1]

[1] Graduate School of Integrated Arts and Sciences, Hiroshima University, Higashi-Hiroshima 739-8521, Japan
[2] Graduate School of Science and Technology, Kumamoto University, Kurokami 860-8555, Japan

E-mail: harada@minerva.ias.hiroshima-u.ac.jp

Abstract
We have carried out hybrid *ab initio*/classical molecular-dynamics simulations for the model system of hydrogen-adsorbed nanostructured graphite. We have investigated the effect of the recrystallization of the nanostructured graphite to the bonding states of hydrogen atoms at 1000 K and the desorption mechanism of the hydrogen dimer from the graphite at 2000 K. We have shown that the recrystallization weakens the bond between the hydrogen and the carbon atoms and the desorption of hydrogen atoms, as the hydrogen dimer occurs at 2000 K.

1. Introduction

Orimo *et al* [1] have found that graphite has the ability to store 7.4 wt% hydrogen ($CH_{0.95}$) after mechanical milling for 80 h under a hydrogen atmosphere [1] and that many nanometre scale defects and vacancies are introduced into the graphite sample during the milling; the resulting graphite sample is called 'nanostructured graphite'. The hydrogen storage capacity of carbon-based materials has attracted much attention in recent years due to their application in fuel-cell energy systems, and many experimental and theoretical studies of hydrogen storage by carbon-based materials such as carbon nanotubes [2] and graphite nanofibres [3] have been reported. Nanostructured graphite is also a candidate hydrogen storage material.

Neutron diffraction measurements [4] suggest that the hydrogen atoms exist in two kinds of state, one is the hydrogen–carbon covalent bond state and the other is the intercalated state between graphite layers. From thermal desorption mass spectroscopy measurements of hydrogen-adsorbed nanostructured graphite, two desorption peaks have been observed at about 750 and 1000 K [5]. This result also suggests that two kinds of hydrogen state exist in the nanostructured graphite. It has been pointed out that the peak at about 1000 K is given by the desorption of the hydrogen atoms bonded chemically with carbon atoms, while the peak at about 750 K comes from the hydrogen molecules absorbed between the graphite layers, though the microscopic mechanism for the desorption of hydrogen atoms has

System
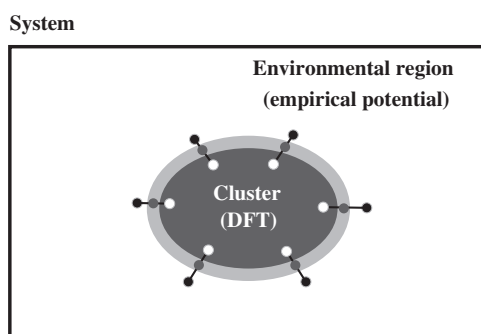
Figure 1. Schematic illustration of the hybrid *ab initio*/classical method. The dark grey and the white regions show the cluster and the environmental region, respectively. The spheres in the light grey region represent the termination atoms.

not been clarified yet [4, 5]. X-ray diffraction measurements [5] of the hydrogen-adsorbed nanostructured graphite show the (002) diffraction peak, which corresponds to the interlayer ordering of the graphite, at 1073 K. It has been pointed out that the diffraction peak shows a recrystallization of the nanostructured graphite, and the desorption peak at about 1000 K is related to the recrystallization. This recrystallization has also been confirmed by differential thermal analysis [5], where an exothermic peak is observed around 1000 K.

In this paper we consider model systems for hydrogen-adsorbed nanostructured graphite, where the hydrogen atoms chemically bond to carbon atoms at the edge of the nanostructured graphite. We apply hybrid *ab initio*/classical molecular-dynamics (MD) simulations based on the density-functional theory (DFT) to these model systems. Our purposes are to investigate (i) the recrystallization of nanostructured graphite and its effect on the adsorbed hydrogen atoms at 1000 K and (ii) the mechanism of desorption of hydrogen atoms at 2000 K.

To simulate the recrystallization of the *nano*structured graphite, bonding between the hydrogen and carbon atoms needs to be treated quantum mechanically and a large model system on a nanometre scale is needed. For these purposes, we use the hybrid *ab initio*/classical MD simulations proposed by Ogata *et al* [6], in which the system is divided into a cluster region and an environmental region. The cluster region is embedded in the environmental region, and atoms in the cluster region are treated by the DFT, while the other atoms are described by the empirical interatomic potential.

2. Method of calculation

In our hybrid *ab initio*/classical MD method [6], the system (referred to as S in the following) is divided into a cluster region (referred to as C), where chemical reactions are assumed to occur, and an environmental region, as shown in figure 1. Atoms in the total system are classified into three types: (i) atoms in the cluster region which are treated quantum mechanically; (ii) atoms in the environmental region which are described by an empirical interaction potential; and (iii) termination atoms which terminate the cluster atoms. The potential energy of the total system is defined as follows:

$$E(r_i \in S) = E_{\text{classical}}(r_i \in S) - E_{\text{classical}}(r_i \in C) + E_{ab\,initio}(r_i \in C), \qquad (1)$$

where r_i is the coordinates of the ith atom, $E_{ab\,initio}$ is the potential energy obtained by the *ab initio* calculation based on the DFT and $E_{\text{classical}}$ is the potential energy calculated using the empirical potential. The potential energy of cluster atoms needs to be calculated by both the
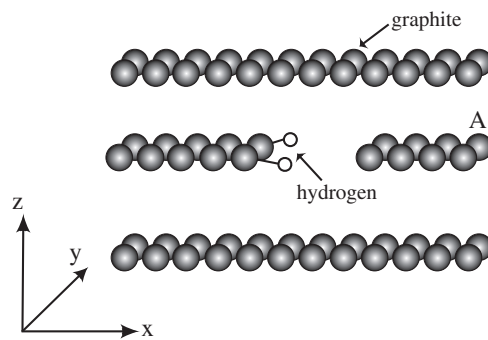
Figure 2. Schematic illustration of the model system. The large grey atoms and the small white atoms denote the carbon and the hydrogen atoms, respectively.

DFT and the empirical-potential calculations. In our hybrid *ab initio*/classical MD simulation, we choose the cluster region such that at least two covalent bonds for each carbon atom are included in the cluster. Since there is a dangling bond for each outermost carbon atom of the cluster, we terminate these dangling bonds. In the *ab initio* calculation, termination atoms are introduced to terminate the dangling bonds of the cluster and their coordinates are given as a function of atomic coordinates in both the cluster and the environmental regions.

In the *ab initio* DFT calculations, the generalized gradient approximation [7] is used for the exchange–correlation energy. The electronic wave functions and the charge density are expanded in plane waves with cut-off energies of 20 and 180 Ryd, respectively. The energy functional is minimized using an iterative scheme based on the preconditioned conjugate-gradient method [8, 9]. The ultrasoft pseudopotential is used for interaction between valence electrons and ions [10]. The Poisson equation is solved with the real-space multigrid method [11] to obtain the Hartree potential, and the local pseudopotential is also calculated in the real space so as to avoid interaction between the periodic replicas.

In the classical empirical-potential calculation, we use the environment-dependent interaction potential (EDIP) proposed by Marks [12]. The EDIP is represented as a sum of the pair potential and the three-body potential, and both of them are the function of not only the distance between two atoms and the angle formed by three atoms for three-body potential, but also the generalized coordination number of the atoms. The potential energy calculated by the EDIP depends on the local environment of the atoms through this generalized coordination number. The EDIP has been applied to the liquid and the amorphous carbon and proved to be able to reproduce the static [12] and the dynamic [13] structures obtained by *ab initio* MD simulations, suggesting a very good transferability of the EDIP. We have also confirmed the validity of our hybrid *ab initio*/classical MD method using EDIP by applying the hybrid method to the graphite sheet (graphene) for investigating the dynamic properties such as heat transfer [13]. In the classical cluster calculation, $E_{\mathrm{classical}}(r_i \in C)$, we introduce carbon atoms as classical termination atoms such that each carbon atom in the cluster region forms three covalent bonds with surrounding carbon atoms. By introducing the termination atoms, three-fold bonding states for all carbon atoms in the cluster are described by EDIP. The three-body contribution mainly comes from these nearest-neighbour covalent-bonding atoms; thus we think that most three-body contribution between the system and the cluster is removed.

Figure 2 shows a schematic picture of the model system of hydrogen-adsorbed nanostructured graphite. The model consists of five graphite layers and the central layer is divided into two separated graphite sheets with armchair edges in order to mimic a defective
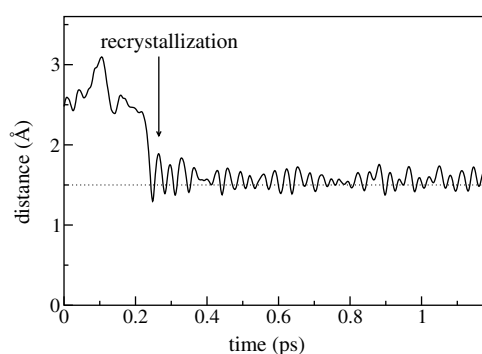
Figure 3. The distance between two carbon atoms in model II.

structure in the nanostructured graphite. Four hydrogen atoms are adsorbed at the edge of the left graphite sheet. The model system contains 1568 carbon atoms and four hydrogen atoms. The hydrogen atoms and the surrounding 32 carbon atoms are considered as the cluster region and are treated by *ab initio* DFT calculation. In the y direction, we apply the periodic boundary condition.

We consider two model systems. First, the gap between the left and right graphite sheets is about 5 Å and there is no interaction between the hydrogen atoms and the right-hand carbon atoms. We carry out the hybrid MD simulation for this system (referred to as model I). The temperature of the system is 1000 K, which is the temperature corresponding to the second peak of the results of the thermal desorption experiment [5]. Next, sheet A in figure 2 is artificially shifted to the $-x$ direction to mimic the recrystallization of the nanostructured graphite, so that the distance between two graphite sheets becomes about 1.5 Å; this is referred to as model II. We carry out the MD simulations for this model at 1000 K. Then, the temperature of the system is raised to 2000 K to carry out further MD simulation. The time step of our MD simulations is 0.97 fs and the simulation is carried out for about 4.5 ps for these models.
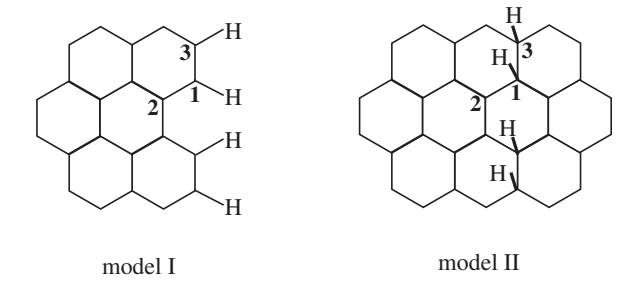
3. Results and discussion

3.1. Recrystallization of the nanostructured graphite

In the MD simulation for model II, the recrystallization of graphite sheets occurs at 0.4 ps after we start the simulation. The recrystallization of graphite sheets means that two graphite sheets combine together to form a single graphite sheet. Figure 3 shows the distance between two carbon atoms which bond together after the recrystallization. After 0.4 ps, the distance of two carbon atoms is about 1.5 Å, which corresponds to the C–C bond length of graphite. Due to the recrystallization, the hydrogen atoms are pushed by both sides of the graphite sheets and move out of the sheet upward or downward.

In table 1 we show the bond lengths, the frequencies of the C–H stretching mode and the bond angles related to the adsorbed hydrogen atoms before (model I) and after (model II) the recrystallization. As is shown in table 1, after the recrystallization, the C–H bond becomes longer and the frequency of the C–H stretching mode becomes lower, which suggests that the bonds between the hydrogen and carbon atoms become weaker. The local structure around the carbon atoms that are connecting with hydrogen atoms also changes due to the recrystallization. After the recrystallization, the C–C bond length between the carbon atom which is bonding with the hydrogen atom and the neighbouring carbon atom becomes longer and the bond angle

4

Table 1. The bond lengths, frequencies of the C–H stretching mode and the bond angles around the carbon atoms which are bonding with the hydrogen atoms.

	Bond length (Å)		Frequency ($\times 10^3$ cm^{-1})	Bond angle (deg)	
	C_1–H	C_1–C_2	C_1–H	H–C_1–C_2	C_2–C_1–C_3
Model I	1.11	1.41	3.05	119.6	119.5
Model II	1.13	1.55	2.76	101.1	116.0

model I

model II

changes from about 120° (three-fold coordinates) to a smaller angle (four-fold coordinates). Note that the C–C bond length in model II is very close to that of diamond, 1.54 Å.

During the recrystallization, the energy of the cluster system gradually decreases. The difference in energy of the system before and after the recrystallization is estimated to be about 0.1 eV/atom. This result shows the possibility of increasing the local temperature of the system due to the recrystallization. Thus, we employ another MD calculation at a higher temperature of 2000 K in the next subsection.

### 3.2. Hydrogen desorption from the nanostructured graphite

After the MD simulation for model II at 1000 K, we continue to carry out the MD calculation at a temperature of 2000 K for 4 ps. The wagging motion of the hydrogen atoms becomes more active than that at 1000 K, and after 0.5 ps, two hydrogen atoms form a hydrogen dimer.

Figures 4(a)–(c) show the time evolution of the electron density distribution around the hydrogen atoms. The contour lines on a plane containing two hydrogen atoms and a carbon atom are drawn at intervals of 2.4×10^{-2} au. At 0.472 ps, two hydrogen atoms are bonding with the carbon atoms, as shown in figure 4(a). At 0.478 ps, two hydrogen atoms are close to each other in figure 4(b), and then two hydrogen atoms form the hydrogen dimer at 0.480 ps as shown in figure 4(c). The dimer is stabilized and moves around between two graphite layers. This result shows that the dimer may desorb from the graphite layers after recrystallization. The bond length and frequency of the H–H stretching mode averaged from 0.5 to 0.9 ps are 0.89 Å and 3.7×10^3 cm^{-1}, respectively.

In these calculations, we need large model systems to simulate the recrystallization of the nanostructured graphite and use the hybrid *ab initio*/classical MD simulations. We have also applied *ab initio* MD simulations for the whole model system after the recrystallization, and we have shown that desorption of hydrogen from the nanostructured graphite and the formation of hydrogen dimers also occur [14].

4. Conclusion

We have applied a hybrid *ab initio*/classical MD simulation to the model system for hydrogen-adsorbed nanostructured graphite to investigate (i) the recrystallization of nanostructured
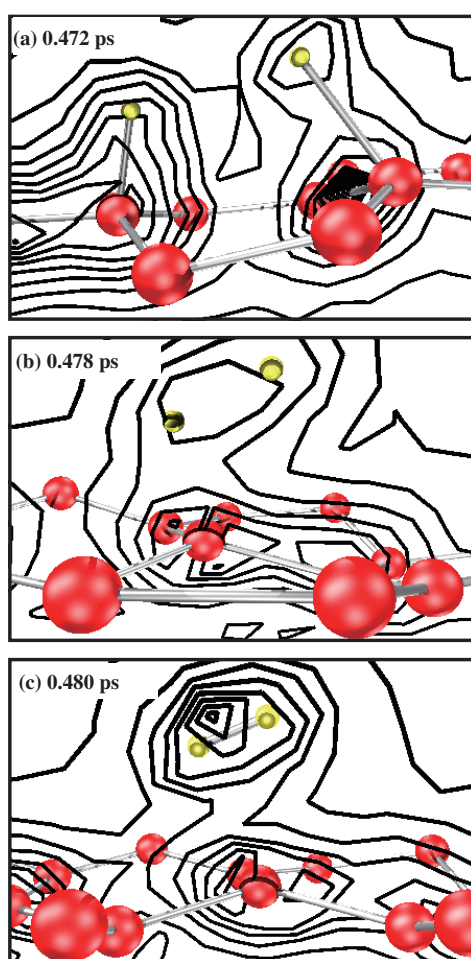
Figure 4. The time evolution of the electron density distribution around the hydrogen atoms at (a) 0.472, (b) 0.478 and (c) 0.480 ps. The big (red) and small (yellow) spheres show the carbon and the hydrogen atoms, respectively. The contour lines are drawn at intervals of 2.4×10^{-2} au.

(This figure is in colour only in the electronic version)

graphite and its effect on the adsorbed hydrogen atoms at 1000 K and (ii) the mechanism of desorption of hydrogen atoms at 2000 K. As a result of the MD simulation, the recrystallization of the nanostructured graphite has been successfully simulated. We have shown that the C–H bonds become weaker due to the recrystallization in the sense that the C–H bonds become slightly longer and the frequency of the C–H stretching mode becomes lower after the recrystallization (model II). Then, we have carried out the MD simulation at 2000 K after the recrystallization and found that two hydrogen atoms form the hydrogen dimer and desorb from the graphite layer. We have investigated the desorption mechanism from the electron density distribution.

Acknowledgments

References

[1] Orimo S, Majer G, Fukunaga T, Züttel A, Schlapbach L and Fujii H 1999 *Appl. Phys. Lett.* **75** 3093
[2] Dillon A C, Jones K M, Bekkedahl T A, Kiang C H, Bethune D S and Heben M J 1997 *Nature* **386** 377
[3] Chambers A, Park C, Baker R T K and Rodriguez N M 1998 *J. Phys. Chem.* B **102** 4253
[4] Fukunaga T, Itoh K, Orimo S, Aoki M and Fujii H 2001 *J. Alloys Compounds* **327** 224
[5] Orimo S, Matsushima T, Fujii H, Fukunaga T and Majer G 2001 *J. Appl. Phys.* **90** 1545
[6] Ogata S, Shimojo F, Nakano A, Vashishta P and Kalia R K 2001 *Comput. Phys. Commun.* **149** 30
[7] Perdew J P, Burke K and Ernzerhof M 1996 *Phys. Rev. Lett.* **77** 3865
[8] Kresse G and Hafner J 1994 *Phys. Rev.* B **49** 14251
[9] Shimojo F, Zempo Y, Hoshino K and Watabe M 1995 *Phys. Rev.* B **52** 9320
[10] Vanderbilt D 1990 *Phys. Rev.* B **41** 7892
[11] Press W H, Teukolsky S A, Vetterling W T and Flannery B P 1992 *Numerical Recipes in Fortran 77: the Art of Scientific Computing* 2nd edn (Cambridge: Cambridge University Press) chapter 19
[12] Marks N A 2001 *Phys. Rev.* B **63** 035401
[13] Harada A, Shimojo F and Hoshino K 2003 *J. Phys. Soc. Japan* **72** 822
[14] Harada A, Shimojo F and Hoshino K 2005 *J. Phys. Soc. Japan* **74** 2270